34th Annual International Conference of the IEEE EMBS
San Diego, California USA, 28 August - 1 September, 2012

Automatic Detection of the Macula in Retinal Fundus Images using Seeded Mode Tracking Approach

Damon W.K. Wong, Jiang Liu, Ngan-Meng Tan, Fengshou Yin, Xiangang Cheng,
Ching-Yu Cheng, Gemmy C.M. Cheung and Tien Yin Wong

Abstract— **The macula is the part of the eye responsible for central high acuity vision. Detection of the macula is an important task in retinal image processing as a landmark for subsequent disease assessment, such as for age-related macula degeneration. In this paper, we have presented an approach to automatically determine the macula centre in retinal fundus images. First contextual information on the image is combined with a statistical model to obtain an approximate macula region of interest localization. Subsequently, we propose the use of a seeded mode tracking technique to locate the macula centre. The proposed approach is tested on a large dataset composed of 482 normal images and 162 glaucoma images from the ORIGA database and an additional 96 AMD images. The results show a ROI detection of 97.5%, and 90.5% correct detection of the macula within 1/3DD from a manual reference, which outperforms other current methods. The results are promising for the use of the proposed approach to locate the macula for the detection of macula diseases from retinal images.**

I. Introduction

The macula is the part of the eye that is responsible for central vision, affecting daily tasks such as reading, driving, and recognition. In color retinal fundus images, the macular region is usually described as a darker region of the retina located temporally to the optic nerve head, and generally growing darker towards the macula centre, due to increased pigmentation. Within the macula is the highest concentration of photoreceptors in the eye. This makes it a key component of visual acuity and color vision.

One of the most common diseases affecting the macula is known as age-related macular degeneration (AMD). AMD has been reported to be 3rd leading cause of blindness after cataracts and glaucoma[1], and is expected to increase in prevalence as the global population ages. In AMD, there is progressive loss of vision as the disease progresses from early stage to late stage. Although research shown that early intervention can be more cost-effective that late stage treatment, there are few visual symptoms in early AMD and very few cases are detected at the early stage. In retinal fundus images however, signs of AMD in the macula region ranging from drusen (early AMD) to geographic atrophy (late AMD) can be observed. Besides AMD, other diseases which affect the macula region include diabetic macular edema, toxoplasmosis, and cherry-red spot.

D.W.K. Wong, J. Liu, N.M. Tan, F. Yin and X. Cheng, are with the Institute for Infocomm Research, A*STAR, Singapore. (e-mail: wkwong@i2r.a-star.edu.sg).

C.-Y. Cheng, G. C.M. Cheung and T.Y. Wong are with the Singapore Eye Research Institute. C.-Y. Cheng and T.Y. Wong are also with the National University of Singapore Health System.

Detection of the macula is thus an important process in retinal image processing, as a key retinal landmark as well as the focal point for disease assessment, particularly in AMD[2]. However, this can be a challenging task, as the macular region does not have a distinctive or well-defined structure such as in vessels or the optic nerve head. Previously, in [3], a template matching approach using a Gaussian blob was used to detect the macula. Cascaded minimum pixel intensity was used to determine the centre of the macula in [4]. A vessel-based point distribution model was to obtain the macula centre, optic nerve head and central arcade in [5].Macula localization was inferred in [6] using detected vessels to determine the raphe along which the macula is likely to occur. More recently, morphological processing was used to detect likely macula blobs in [7].

In this paper, we propose to automatically detect the macula centre using the aggregation of seeded mode tracking in retinal fundus images. The approach is fully described in Section II. In Section III, we present the results of our experiments on a large dataset of 796 images and conclude our findings in Section IV.

II. Method

In our method, we first perform pre-processing to determine and remove un-useable areas of the image. Using a detected optic disc, we then identify if the image belongs to a left or right eye. Using this information, an approximate region of interest around the typical macula location is extracted. This region is used for our proposed seeded mode searching approach to detect the macula.

A. Preprocessing

The quality of an image is an important consideration for image analysis. In a retinal fundus image, as in Figure 1, an

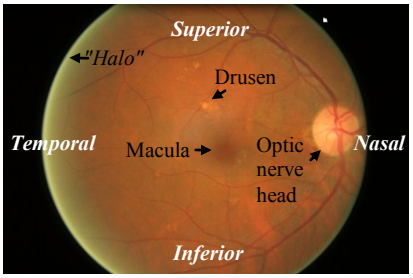

Figure 1. Retinal fundus image of a right eye. Black text describe retinal features, while white text refer to clinical nomenclature to describe positioning in the eye.

imaging artifact commonly observed is the presence of a halo around the fundus field of view. This is caused by optical misalignment between the eye and the optical system of the camera when the eye shifts during the image acquisition process. Further, due to defocusing or cataracts, regions of the retina fundus image can appear hazy or blurred. In clinical practice, the gradeability of an image is determined by the visibility of vessels within that image. We adopt this criterion to determine the useable regions of the image for further processing in our approach. Using the green channel, where vessels are most obvious, vessels are first detected using a vessel detector based on the morphological black top-hat transform, similar to that used in [8]. This is defined as the difference between the morphological closing of an image and the input image, with the structuring element is defined by the size of the largest expected vessel diameter. The result of this operation is a binary mask containing an approximate segmentation of the retinal vessels, and the circular field of view is shifted to inwards to only consider the region bounded by the detected vessels. This results in exclusion of hazy regions as well as the exterior halo.

B. Optic disk landmark

The optic disk is a highly visible features in a fundus image. Also known as the optic nerve head, it is the part of the retina from which vessels and retinal nerve fibers exit, and can be visually described as an elliptical region of higher intensity compared to the surrounding retina. A region-growing method is used to detect the optic disk. We use our previously reported approach based on the active shape model to detect the location of the optic disk.

C. Macular ROI Detection

Compared to the optic disk, the macula is less distinct. It can be visually described as a region with a gradual decline in intensity levels with no obvious boundaries. Detection of the macula is thus prone to noise and local variations. To enhance detection, we define a macular region of interest (ROI) . This ROI is modeled on the spatial relationship between the optic disk and macula, which can be learnt from prior experimental and observed data. However, the proper extraction of the macular ROI also requires knowledge of the orientation of the eye, i.e. if the image is from a left eye, the macula is displaced to the right of the optic disc, and is displaced to the left of the optic disc in a right eye.

To identify the orientation of the eye, we studied the characteristics of the optic disk and made the following observations. In a typical left eye, vessels in the optic disk are denser in the left (nasal) side than the right (temporal) side. Correspondingly, the optic disk is generally of higher intensity towards the right half of a left eye, due to the lack of vessels in that half. We derived the following rules. Let S_L be the set of pixels in the left half of the optic disk, and S_R be the set of pixels in the right half of the optic disk. Also, let G refer to the green channel of the image, and V be the detected vasculature mask. For a left eye, we define

Rule 1) $G(S_R)>G(S_L)$
Rule 2) $V(S_R)<V(S_L)$

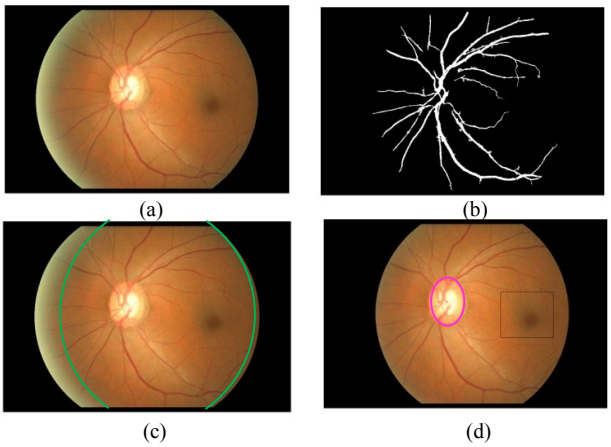

Figure2. (a) Input image, (b) vessel detection, (c) halo filtering with adjusted field of view defined by the green contours and (d) optic disc detection (magenta ellipse) and macula ROI (black box)

The rules are reversed for a right eye. Additional adjudication can be provided by using the relative position of the optic disk in the image, however based on our experiments this is rarely necessary.

Using prior data, we statistically determined the average unsigned distance (μ_x,μ_y) of the macula with respect to the optic disk centroid, along with the range of variation (Δx, Δy), as follows, using the orientation information,

$$X = \begin{cases} \{x \in \mathbb{Z}^+ : x = x_{OD} + \mu_x \pm \Delta x\}, & \text{left side} \\ \{x \in \mathbb{Z}^+ : x = x_{OD} - \mu_x \pm \Delta x\}, & \text{right side} \end{cases}$$

$$Y = \quad \{y \in \mathbb{Z}^+ : y = y_{OD} + \mu_y \pm \Delta y\}$$

X,Y represent the range of coordinates for ROI extraction, and γ represents an additional buffer margin, and x_{OD}, y_{OD} represent the x and y coordinates of the optic disk centroid respectively. An example is shown in Figure 2.

B. Seeded Mode Tracking for Macula Detection

Compared to other structures in the retina, the macula is less well defined and tends to have no obvious boundaries. Visually, it is observed to be generally darker compared to the surrounding retina, particularly in the green channel. Although a simple method would be to simply locate the darkest region or spot in the macula ROI, often this can be confounded by the presence of retinal vessels, which also appear dark, and potentially darker than the retina. In addition, in some retinas, the thinning of the retinal layer reveals the underlying choroidal vessels, which also results in intensity variation.

We propose a seeded mode seeking approach which attempts to locate the macula by tracking the aggregation of independent seeds. To reduce the effect of vessels during tracking, we perform morphologically opening using a structuring element based on the largest vessel diameter on the ROI during initialization. We define an initial grid of n x n seeds equally distributed in the macula ROI at time t = 0.

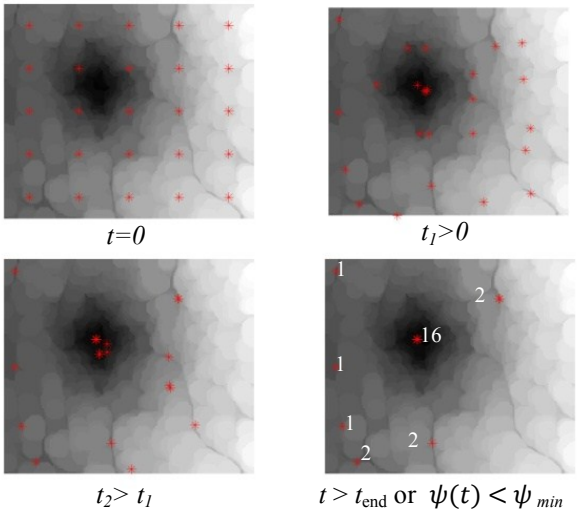

Figure 4. Seeded tracking process from initialization (t = 0), towards convergence (t_1,t_2) and at convergence when

At t = 1, each seed begins to search its r x r pixel neighbourhood, where r is defined as the minimum distance between each seed at initialization. The local minimum in its neighbourhood is found and the seed moves to that location. Subsequently, at the next time step, the seed again searches the new r x r neighbourhood and moves to the local minimum. The tracking process method is repeated for each seed, and termination occurs when $t > t_{\text{end}}$ or when $\psi(t) < \psi_{min}$ where

$$\psi(t) = \sum_{j=1}^{N} \left| \mathbf{x_j}(t) - \mathbf{x_j}(t-1) \right|$$

N refers to the total number of seeds, $\mathbf{x_j}(t)$ refers to the coordinates of the seed at time t, and ψ_{min} is the cutoff value which for the total seed movement, and is used to avoid local oscillations.

At tracking termination, the seeds aggregate in certain locations representing regions of local minima. Seeds which are less than r pixels apart are combined into a single median location. We use the aggregated location which the largest number of seeds as detected macula location. This approach has the advantage of using the collective decision of multiple seeds for macula detection based on majority voting, rather than through the use of single pixel values which are highly prone to false detections. Figure 3 illustrates the process.

III. Experiments and Results

To evaluate our proposed automatic method for macula detection, we used the ORIGA [9] dataset and an additional dataset of images with age-related macular degeneration from the Singapore Eye Research Institute. ORIGA consists of a set of 650 retinal fundus images composed of 168 images from glaucoma eyes and 482 images from normal eyes. These images were acquired using a 45° FOV Canon CR-DGi retinal fundus camera with a 10D SLR backing, with an image resolution of 3072x2048 pixels. The AMD dataset consists of 96 images captured using the same equipment and imaging protocol. To mark the macula centre, we developed a marking tool and the macula was marked by an expert using this tool, and used as the reference for subsequent comparison.

We tested our proposed system using the full dataset of 746 retinal images (482 normal eyes, 168 glaucoma eyes and 96 AMD eyes). Selected results are shown in Figure 5. As a form of comparison, we also conducted experiments in which the macula was assumed to be located in the centre of the macula ROI (*CenROI*), and when a simple search of the ROI minimum was used for macula detection (*MinROI*). In addition, we tested our previously reported method (*Morph*) from [7] on the dataset. Performance of these methods were evaluated by calculating the Euclidean distance D between the reference macula location and the location of the macula obtained from the various methods. The average μ_D and mean statistics σ_D of the experiments are presented in Table I. To further assess the results, we included an additional criterion based on the AREDS macular-focused grading protocol[2]. In the AREDS grading graticule, the inner circle used for centering on the macula has a radius of 1/3DD, where DD is the typical optic disc diameter (DD). We used this to determine 'correct' macula detection with respect to the reference macula location. DD was based on the reference optic disc diameters in the dataset.

The results show that our approach has a high success rate in detecting the macula centre across different normal, glaucoma and AMD eyes. In macula ROI extraction, our proposed approach was able to correctly determine the ROI containing the macula in 97.5% of the dataset. In the cases when the ROI was incorrectly detected, the two main causes were observed be the wrong detection of the optic nerve head, as well as atypical distribution of the optic nerve head vasculature and pallor distribution. However, it should be noted that these occur only in a small proportion of the images tested.

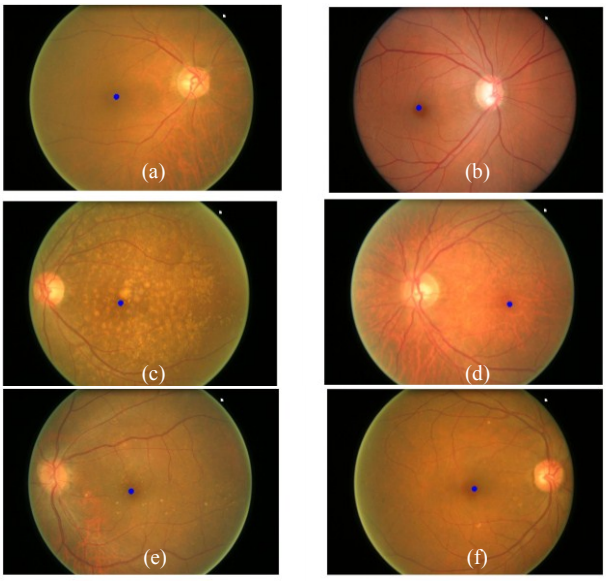

Figure 5. Detected macula (blue spot) in an retinal image from a (a) normal eye, (b) glaucoma eye, (c) AMD eye with small soft drusen, (d) AMD ee with larger but few drusen, (e) AMD eye with large, numerous drusen and (f) AMD eye with thin RPE layer revealing underlying choroidal vessels

TABLE I. EXPERIMENTAL RESULTS FOR MACULA DETECTION

Dataset	Method	Correct ROI detection	Macula detected within 1/3DD of reference		
			# (%)	μ_D	σ_D
Normal	*Proposed*	473 (98.1%)	432 (91.3%)	33.48	23.23
482	*CenROI*		428 (90.5%)	62.19	27.84
	MinROI		410 (86.7%)	32.37	21.43
	Morph		400 (84.6%)	30.34	21.77
Glaucoma	*Proposed*	161 (95.8%)	139 (86.3%)	39.22	28.36
168	*CenROI*		135 (83.9%)	62.28	28.63
	MinROI		130 (80.8%)	39.77	27.89
	Morph		119 (73.9%)	34.47	24.28
AMD	*Proposed*	94(97.9%)	86 (92.5%)	37.15	25.65
96	*CenROI*		74 (79.6%)	66.25	30.22
	MinROI		81 (87.1%)	38.28	24.80
	Morph		83 (89.3%)	33.57	27.39
Overall	*Proposed*	727 (97.5%)	656 (90.3%)	35.19	24.82
746	*CenROI*		637 (87.6%)	62.01	28.29
	MinROI		621 (85.4%)	34.69	23.55
	Morph		601 (82.7%)	31.56	23.15

Our approach was also able to correctly localize the macula with a higher accuracy than the other methods tested. Using the same macula ROI as an input, our proposed approach achieved the highest rate of correctly detected macula centres, defined to be within 1/3DD of the reference macula localization. Although other methods such as *Morph*

Our approach was also able to correctly localize the macula with a higher accuracy than the other methods tested. Using the same macula ROI as an input, our proposed approach achieved the highest rate of correctly detected macula centres, defined to be within 1/3DD of the reference macula localization. Although other methods such as *Morph* [7] was able to achieve a lower average error μ_D, this was at the expense of a 7.6% reduction in the macula detection rate.

The results also show that the although the statistical average macula location *(CenROI)* can give a stable approximate macula location, but the actual error distance is nearly twice that of our proposed rate. In contrast, the use of a global minimum detector (*MinROI*) allows greater freedom in detecting the macula, but also a greater risk of false detection.

IV. CONCLUSION

We have presented a method for the detection of the macula centre in retinal fundus images. In our approach, we localize the macula region of interest using statistical priors with the context of the side of the eye. Next, we applied a seeded mode tracking approach to obtain the macula centre. Experiments of a large set of 746 images from normal, glaucoma and AMD eyes in comparison with other methods show that our approach is promising and achieves a successful detection in 90.3% of the images. The results are encouraging for the use of this approach in the automated analysis of macular-related pathologies.

REFERENCES

[1] D. Pascolini, S.P. Mariotti, G.P. Pokharel, R. Pararajasegaram, D. Etya'ale, AD. Negrel, and S. Resnikoff, "2002 global update of available data on visual impairment: a compilation of population-based prevalence studies", *Ophth. Epid.*, 2004, 11, (2), pp. 67-115.

[2] Age-Related Eye Disease Study Research Group, "A simplified severity scale for age-related macular degeneration," *Arch Ophthalmol.* 2005;123:1570–1574.

[3] C. Sinthanayothin, J. Boyce, H. Cook, and T.Williamson, "Automated localisation of the optic disc, fovea, and retinal blood vessels from digital colour fundus images," *Br. J. Ophthalmol*., vol. 83, pp. 902–910, 1999.

[4] L. Gagnon, M. Lalonde, M. Beaulieu, and M.-C. Boucher, ''Procedure to detect anatomical structures in optical fundus images,'' in *Proc. SPIE*, 2001, pp. 1218–1225.

[5] M. Niemeijer, M. D. Abramoff, and B. v. Ginneken, "Segmentation of the optic disc, macula and vascular arch in fundus photographs," IEEE Trans. Med. Imag., vol. 26, no. 1, pp. 116–127, Jan. 2007.

[6] K.W.Tobin, E. Chaum, V.Priyag gvindasamy, and T.P.Karnowski, "Detection of Anatomic Structures in Human Retinal Imagery," *IEEE Trans. Med. Imag.*, vol.26, no.12, pp.1729-1739, Dec. 2007.

[7] N.M. Tan, J. Liu, D.W.K. Wong, Z. Zhang, S. Lu, J.H. Lim, H. Li and T.Y. Wong, "Classification of left and right eye retinal images", *Proc. SPIE* 7624, 762438 (2010).

[8] C. Muramatsu, Y. Hatanaka, T. Iwase, T. Hara, H.Fujita, "Automated detection and classification of major retinal vessels for determination of diameter ratio of arteries and veins", *Proc. of SPIE* Vol. 7624 76240J-1.

[9] Z. Zhang Z, F. Yin, J. Liu, D.W.K.Wong, N.M. Tan, B.H. Lee, J. Cheng, T.Y. Wong, "ORIGA(-light): an online retinal fundus image database for glaucoma analysis and research," *Conf Proc IEEE Eng Med Biol Soc*. 2010;2010:3065-8.